



Semnan University

Mechanics of Advanced Composite Structures

journal homepage: <http://MACS.journals.semnan.ac.ir>

Study of Bond Strength between Polymer-Modified Mortars/Concrete and Their Mechanical Properties using “Friction-Transfer” and “Pull-off” Methods

A. Saberi Varzaneh*, M. Naderi

Department of Civil Engineering, Imam Khomeini International University, Qazvin, Iran

KEYWORDS

Polymer-modified mortar
Semi-destructive tests
Mechanical properties
Finite element method
Adhesion

ABSTRACT

Nowadays, polymers in cement-based mortars are frequently used to improve mechanical properties and increase the adhesion between the repair mortar and concrete substrate. In the present study, the mechanical properties of the polymer-modified mortars in the various ages were evaluated using the semi-destructive and in-situ “friction-transfer” and “pull-off” tests. For this purpose, the repair mortar was prepared with various styrene butadiene rubber (SBR) latex-cement ratios (10, 15, and 20%) and tested at 7, 42, and 90 days of age. The correlation between the results from semi-destructive tests and the compressive and flexural strengths of mortars were determined. The calibration diagrams were presented to determine the mechanical properties of the mortars. Also, the effect of the polymer was investigated on the shrinkage and bond strength between mortars and concrete substrate. Finally, the stress and cracks obtained from the “friction-transfer” and “pull-off” tests were presented using the finite element analysis software (ABAQUS). There was excellent congruence between the results from the above tests and the finite element analysis. There was a high correlation between the results of the “friction-transfer” and “pull-off” tests. Therefore, the simple and inexpensive “friction-transfer” device can be used instead of the expensive “pull-off” device. Besides, the significant correlation between the mechanical properties of the polymer-modified mortars and the above tests shows the suitability of the semi-destructive methods in investigating the mechanical properties of the mortars.

1. Introduction

Polymer-modified mortars (PMM) refer to mortars that are mainly bound using cement, while polymers are also added to them to improve some of their mechanical, physical, and chemical properties. Nowadays, due to their good adhesion and low permeability, PMM are used as repair materials in damaged parts of concrete elements. Styrene-butadiene rubber (SBR) latexes are cheap polymers that are readily available in large quantities. Adding SBR to repair mortars increases their flexural strength, while having no positive effect on their compressive strength [1, 2]. The reason behind the reduced compressive strength of SBR-modified mortars compared to ordinary ones is the increased pores and air bubbles in them [3]. A study on the effects of vinyl acetate-ethylene polymer on repair mortars showed that with the rise in the volume

of the polymer, the flexural strength increased at first and then decreased, while the compressive strength was reduced linearly [4].

Other advantages of using polymers include the reduction in the density [5] and permeability [6] of the mortars, and a rise in the bond strength between the mortar and the substrate [7]. In a study on the effects of vinyl acetate-ethylene polymer on the shrinkage and adhesion of repair mortars, this polymer was found to have no significant impact on shrinkage, while increasing the adhesion between the mortar and the substrate [8]. Another study investigating the effects of creating an interface between the substrate and the styrene acrylic emulsion-modified mortar revealed that making the interface rougher increased the strength of the bond [9]. In a study on the effects of acrylate polymer (AC), polyvinyl alcohol (PVA), styrene-butadiene rubber (SBR), and ethylene-vinyl

* Corresponding author. Tel.: +98-912-2962516
E-mail address: ali.saberi@edu.ikiu.ac.ir

acetate (EVA) polymers on the flexural and adhesive strengths of repair mortars, the highest rise in the flexural strength, i.e., 63%, was observed in the mortars modified with ethylene-vinyl acetate. The other polymers increased the flexural strength of the mortars by 16% to 46%. Moreover, the SBR-modified mortars had the highest bond strength [10]. A study on the effects of styrene-butadiene rubber and acrylate polymers on the adhesive strength of concretes as a repair layer showed that the SBR provided a higher adhesion, and the optimum amount of polymer in the concrete was 20% of the cement weight [11].

In a study on the flexural strength of the styrene-butadiene rubber (SBR) polymer modified mortars and also the adhesion of these mortars on the substrate concrete, it was found that adding 5% SBR polymer leads to a 25.2% increase of flexural strength and a 46.7% increase of adhesion. Also, adding 15% polymer leads to a 65% increase in flexural strength and a 77% increase in adhesion [12]. It was observed in another study that SBR polymer increases flexural strength and decreases mortar shrinkage such that the shrinkage of the mortars with 10% polymer was equal to 0.026 while adding 20% polymer led to 0.021% shrinkage [13]. By adding different ratios of SBR polymer equal to 2.5, 5, 10, 15, and 20% to the repair mortars in a study, it was observed that the compression strengths of the mortars were decreased by increasing the amount of the polymer [14]. It was observed in another study that adding SBR polymer increases adhesion strength between the mortar and the substrate concrete such that the adhesion between a usual mortar and concrete is equal to 1.3MPa while the adhesion between the polymer modified mortar and substrate concrete is equal to 2.4MPa [15]. It was observed in another study that SBR polymer, in addition to increasing the adhesion between mortar and substrate concrete, causes a 15% decrease of shrinkage in mortars [16]. Another study showed that adding SBR polymer increases the adhesion between mortar and substrate concrete up to 60% [17]. Also, adding 20 and 15% SBR polymer leads to the decreases of shrinkage in cement mortars equal to 56 and 44% respectively [18].

Polymers are also used to reinforce the structural elements of the concrete. In a study, fiber-reinforced polymers were used to strengthen steel-reinforced concrete beams [19]. The results showed that the load-bearing capacity of the reinforced beams was 30% to 98% more than that of ordinary concrete beams. Furthermore, using perlite mortar with a thickness of 50 mm on fiber-reinforced polymer beams resulted in resistance to the temperature of 500°C for up to three hours [20]. An

experimental and finite element study indicated the increased probability of segregation of the fiber-reinforced polymers and the concrete [21]. By functionalizing the isocyanatoethyl methacrylate polymer in a study, it was found that the product turned into a membrane, which could be effectively used as an adhesive [22].

The tests performed on cementitious materials have mostly been laboratory ones. However, in-situ tests should be used to evaluate the mechanical properties of cementitious materials, while considering the temperature and moisture conditions of a structure. These tests are classified into non-destructive, semi-destructive, and destructive categories. The Schmidt hammer [23] and ultrasonic [24] tests are in the non-destructive category. Destructive tests include coring [25] and pull-out [26] tests. In addition, the pull-off [27], friction-transfer [28], and twist-off [29] tests are in the semi-destructive category.

In this study, in-situ friction-transfer and pull-off tests were employed to measure the bond strength between the polymer-modified mortars and the concrete substrate, and to evaluate the compressive and flexural strengths of the mortars. At first, the correlation coefficients between the results obtained from in-situ and laboratory tests were determined to evaluate the mechanical properties of the polymer-modified mortars. Then, the calibration curves were plotted. The effects of styrene-butadiene rubber (SBR) latexes on the shrinkage of the mortars and the bond strength between the substrate and the mortar were also evaluated. Finally, by modeling the friction-transfer and pull-off tests in ABAQUS, the experimental and numerical results were compared.

2. Experimental works

2.1. Materials

Portland cement type II with a density of 3007 kg/m³ was used to make the concrete for the substrate and the repair layers. According to ASTM C128 [30] and ASTM C127 [31], the water absorption of gravel and sand is 2.6% and 3.2%, respectively. The densities of the gravel and sand in the saturated-surface-dry form are 2330 kg/m³ and 2510 kg/m³, respectively, while their maximum particle sizes are 19 mm and 4.75 mm, respectively. The Sand and gravel were granulated based on the ASTM C136 standard [32]. Fig. 1 depicts their grain size distribution curve. The polymer used to modify the mortars was styrene-butadiene rubber (SBR). A poly-carboxylate super plasticizer was used to make the substrate concrete.

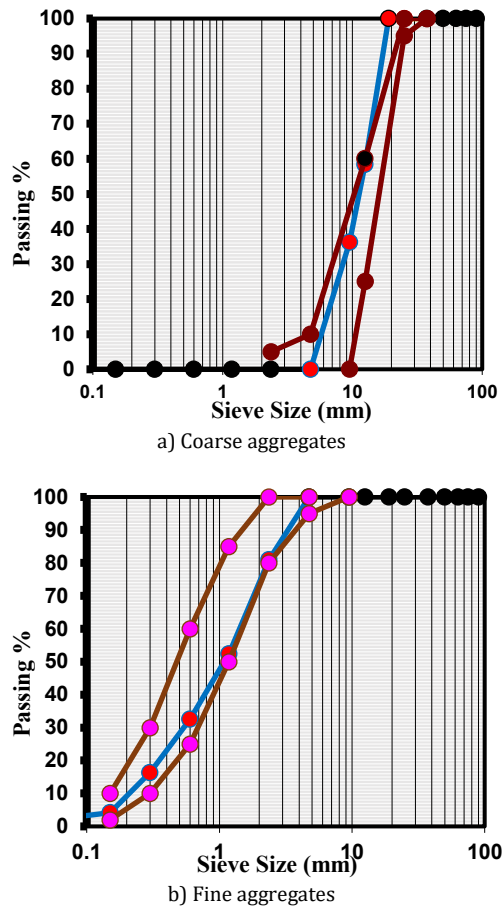


Fig. 1. The granulation diagram of the aggregates

In the pull-off tests, a two-part epoxy resin adhesive was used to attach the steel cylinder to the surface of the mortar. Table 1 lists the mechanical properties of the adhesive based on the product’s catalog provided by the manufacturing company.

2.2. The mortars and substrate concrete

The repair layers were made with a sand to cement ratio of 2 and a water to cement ratio of 0.5. The polymer-modified repair mortars had different amounts of polymer, i.e., 10%, 15%, and 20% of the cement weight. The mix designs of the substrate concrete were determined using the National Method for Concrete Mix Design [33]. The 28-day compressive strength of the specimens was obtained as 57MPa. Table 2 presents the mix designs of the concrete substrate.

2.3. Making the samples and experimental methods

The substrate concrete was 150 mm in length and width with a height of 50 mm. In order to make the substrate concrete, 150*150*150 mm³ cubic concrete specimens were made. Then, using a concrete saw, each specimen was divided into three similar parts, as shown in Fig. 2.

Table 1. Mechanical Properties of Epoxy Resin Adhesive (catalog of manufacturing company)

Modulus of Elasticity	7-Day Compressive Strength	Shear Strength	Setting Time		Curing Time	
			35oC	25oC	35oC	25oC
12750 MPa	70 MPa	15 MPa	4 h	10 h	45 min	90 min

Table 2. Substrate Concrete Weight Ratios (kg/m³)

Cement	Gravel	Sand	Water	W/C Ratio	Superplasticizer
534	664	835	187	0.35	2.61

In order to make the repair layer, the substrate concrete was first put in the mold. Then, the cement grout was poured onto the substrate’s surface, and a repair layer with a height of 25 mm was applied over it (Fig. 3). The adhesion specimens were cured for seven days in water. According to ASTM C157 [34] and ASTM C490 [35], cylindrical specimens with a height of 285 mm and a square section of 25 mm should be employed to measure the shrinkage of the repair mortars. Moreover, the measuring piece should be 250 mm in length. The length comparer for determining the length variation of the specimens should be designed in such a way that a specimen can be placed in it while having complete and proper contact with the test shear studs (Fig. 4). According to ASTM C109 [36], 50*50*50 mm³ cubic specimens were prepared and placed under a compression machine to

measure the compressive strength of the repair mortar. Moreover, 40*40*160 mm³ prismatic specimens were prepared for flexural tests according to ASTM C190 [37]. These specimens were kept in water until performing the tests.



Fig. 2. Cutting the substrate concrete



Fig. 3. Applying the grout and the repair layer over the concrete substrate



Fig. 4. Shrinkage test

According to Fig. 5.a, to determine the bond shear strength between the repair mortar and concrete substrate, a small core is made on the surface of the repair mortar primarily so that the core depth continues into the concrete substrate about 10 mm. Afterward, the metal machine of “friction-transfer” test is stabilized on the core and the torsional moment was applied using torque meter so that the core was separated from the substrate. According to Fig. 5.b, to evaluate the mechanical properties of the mortars, the 150 mm cubic samples were made and then a core with 50 mm of diameter and 25 mm of height was made on the surface of the sample using the core-drilling machine. Afterward, the metal machine is stabilized on the core and the core was fractured by applying the torsional moment to it.

In the “friction-transfer” method, the fractured core was cylindrical with the circular cross-section. Therefore, according to Fig. 6.a, by applying the torsional moment to the cylindrical core, the maximum shear stress occurs on the circumference of circle, which has the farthest distance from the center. In this state, relation 1 can determine the maximum value of the shear stress applied by the torque.

$$\tau_{E-\max} = \frac{T r}{J}, J = \frac{\pi r^4}{2} \rightarrow \tau_{E-\max} = \frac{2T}{\pi r^3} \quad (1)$$

Where r is the radius of core and J is the second polar moment of surface.

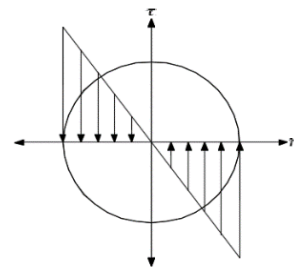


a) Determining the Bond shear strength

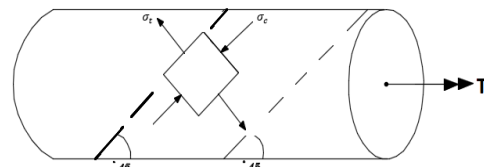


b) Evaluating the mechanical properties

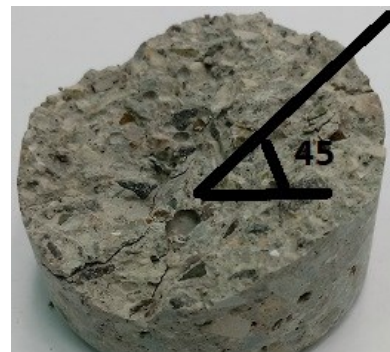
Fig. 5. The “friction-transfer” test



a) The principal stress



b) The angle of fracture



c) The core fracture

Fig. 6. The theory of “Friction-Transfer”

According to the Mohr's circle, it is concluded that the principal compressive and tensile stress make a 45 degrees angle with the horizon. Considering the brittle materials, such as mortar,

have the tensile fracture, therefore, as the Fig. 6.b illustrates, the fracture planes are perpendicular to the tensile stress direction. Fig. 6.c demonstrates that the core fracture in the “friction-transfer” test has an angle of about 45 degrees with the horizon.

The “Pull-off” test, was also employed to measure the bond shear strength and evaluation of in situ mechanical properties of mortars. To measuring the adhesion, a core was made in the surface of the repair mortar and it continues up to a height of 10 mm into the substrate surface. Afterward, the metal cylinder is attached to the core using epoxy resin adhesive, and the force is applied to it by the puller machine until the core was separated from the substrate surface (Fig. 7.a). In addition, to evaluate the mechanical properties of the mortars coring, the metal cylinder is attached on the surface of the sample, and then by applying the tensile force, the mortar was fractured and separated from the cylinder (Fig. 7.b). Table 3 lists the tested specimens, the number of specimens, their dimensions, and the ages at which they were tested.



a) Determining the bond tensile strength



b) Evaluating the mechanical properties

Fig. 7. The “Pull-off” test

Table 3. Made samples

Samples	Number	Dimension (mm)	Test age (Day)
Concrete substrate	48	150*150*50	7, 42, 90
Repair mortar	48	150*150*25	7, 42, 90
Compressive strength	72	50*50*50	7, 42, 90
Flexural strength	36	40*40*160	7, 42, 90
In-situ methods	48	150*150*150	7, 42, 90
shrinkage	60	25*25*285	7, 14, 28, 42, 90

3. Results and their analysis

3.1. Evaluation of the mechanical properties using in-situ tests

This section evaluates the relationship between the results obtained from in-situ tests and the mechanical properties of the mortars using linear and exponential regression analysis. The linear regression curve passes through the origin of the coordinates to measure the coefficient of determination between the compressive strength of the mortars and the in-situ test results. Moreover, since the relationship between the compressive and flexural strengths is exponential, the relationship between the in-situ tests and the flexural strengths of the mortars was evaluated using exponential regression analysis.

3.1.1. Results of the friction-transfer Test

Fig. 8 depicts the relationship between the compressive strength of the mortars and the results of the friction-transfer test.

According to Fig. 8, the coefficient of determination in the linear mode is 0.9518; however, when the curve passes through the origin, the coefficient is 0.9517. As can be seen, a slight difference exists between the coefficients of determination. Therefore, the compressive strength of the PMM can be determined using friction-transfer tests and the equation $y=0.113x$.

In a study on the relationship between the compressive strength of the concrete and the friction-transfer test results, coefficients of determination of more than 90% were observed [28]. This study also showed that the coefficient of determination between the compressive strength of the mortars and the friction-transfer test results was 95%.

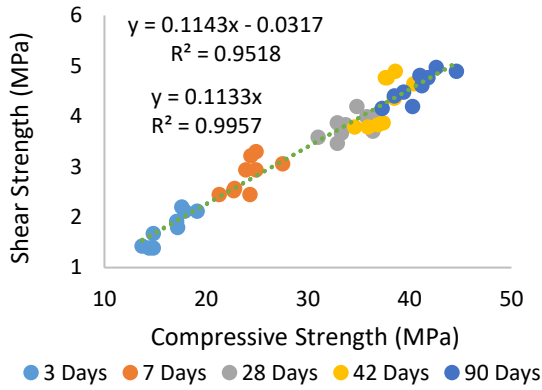


Fig. 8. Correlation between compressive strength and results of “friction-transfer” test

Fig. 9 depicts the relationship between the flexural strength of the mortars and the results of the friction-transfer test.

According to Fig. 9, it is observed that the coefficients of determination equal to 0.77. Therefore, the flexural strength of the PMM can be determined using friction-transfer tests and the equation $y = 0.039^{1.79}$.

3.1.2. Results of the “Pull-off” test

Fig. 10 depicts the relationship between the compressive strength of the mortars and the results of the pull-off test.

According to Fig. 10, the coefficient of determination in the linear mode is 0.9473; however, when the curve passes through the origin, the coefficient is 0.9449. As can be seen, a slight difference exists between the coefficients of determination. Therefore, the compressive strength of the PMM can be determined using pull-off tests and the equation $y=0.063x$.

Fig. 11 depicts the relationship between the flexural strength of the mortars and the results of the pull-off test.

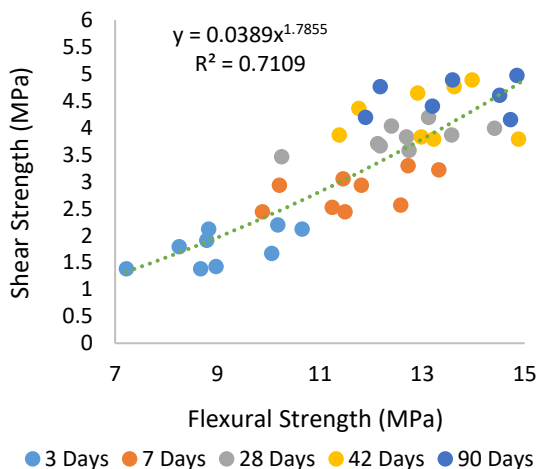


Fig. 9. Correlation between flexural strength and results of “friction-transfer” test

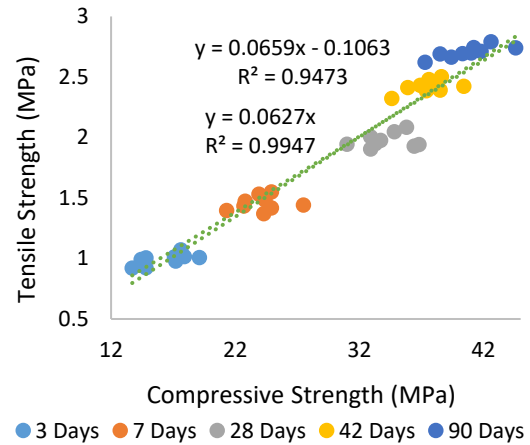


Fig. 10. Correlation between compressive strength and results of “Pull-off” test

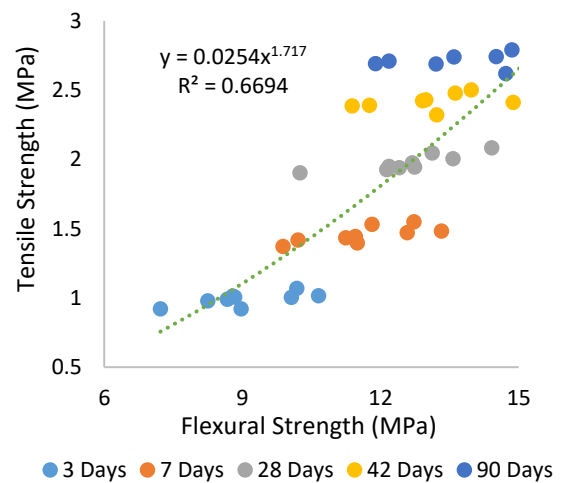


Fig. 11. Correlation between flexural strength and results of “Pull-off” test

According to Fig. 11, it is observed that the coefficients of determination equal to 0.725. Therefore, the flexural strength of the PMM can be determined using pull-off tests and the equation $y = 0.025^{1.717}$.

3.2. Shrinkage of polymer-modified repair mortars

This section evaluates the shrinkage of repair mortars at different ages. The effects of different percentages of polymer on the PMM are also discussed. Fig. 12 presents the shrinkage curve of the mortars. As can be seen from Fig. 12, higher volumes of polymer in the mortars reduced the shrinkage. The shrinkage of ordinary mortars at the age of 90 days was 0.082%, while the shrinkage of the PMM with 10%, 15%, and 20% polymer was 0.056%, 0.051%, and 0.047%, showing 31%, 37%, and 43% reduction in shrinkage, respectively. Moreover, the shrinkage reduced significantly as the percentage of the polymer increased. Similar results have been reported in other studies.

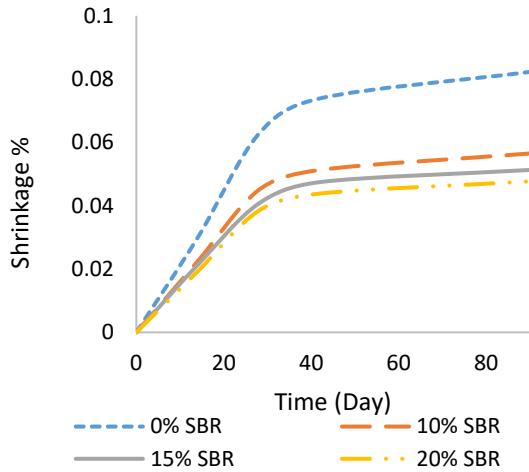


Fig. 12. The mortars' shrinkage

Different study on the effect of SBR latex had also concluded that adding polymer reduces the dry shrinkage [38]. One of the main reasons in the shrinkage decrement of the polymer-modified mortars is the sealing property of latex that prevents the humidity output from the inside of the cement matrix [39-40].

3.3. Bond strength

3.3.1. Bond shear strength obtained from the "friction-transfer" test

Fig. 13 demonstrates the bond shear strength between repair mortars and the concrete substrate obtained from the "friction-transfer" test.

Fig. 13 shows that adding 10% of SBR latex to the mortar increased the bond shear strength within the ages of 7, 42, and 90 days by 35.9, 141.7 and 209.7%, respectively. Also, by adding 15% of SBR latex, the adhesion increment in the mentioned ages was equal to 58.7, 184.8 and 269.9%, respectively. The bond shear strength increment is also observed by adding 20% of SBR latex so that the bond strength increment within the ages of 7, 42, and 90 days was equal to 49.1, 167.5 and 250.3%, compared to the polymer-free mortar, respectively.

However, as can be seen, adding 20% polymer had a smaller effect compared to adding 15% polymer since the SBR latex created air bubbles inside the cementitious material's structure, creating porosity in the mortar [41]. Therefore, larger increases in the amount of polymer can have adverse effects.

Similar results have been observed in other studies, where the addition of SBR latex increased the bond strength between the mortar and the substrate [42]. The rise in the adhesion in such mortars is due to the formation of polymer films. When a polymer has contact with the cement paste, the strong covalent or ionic bonds

give more cohesion to the entire matrix, improving adhesion [43].

3.3.2. Bond tensile strength obtained from the "Pull-off" test

Fig. 14 shows the bond strength between the concrete and the polymer-modified mortars based on the pull-off tests.

As can be seen from Fig. 14, at the age of 90 days, the rise in the adhesion of the mortars containing 10%, 15%, and 20% polymer was equal to 170.2%, 220.3%, and 201.3%, respectively. The corresponding values were 94.8%, 125.7%, and 113.2% at the age of 42 days, and 31.4%, 56.7%, and 44.8% at the age of 7 days, respectively.

However, as can be seen, adding 20% polymer had a smaller effect compared to adding 15% polymer since the SBR latex created air bubbles inside the cementitious material's structure, creating porosity in the mortar [41]. Therefore, larger increases in the amount of polymer can have adverse effects. Fig. 15 shows the correlation between bond shear strength obtained from the "friction-transfer" test and bond tensile strength obtained from the "pull-off" test.

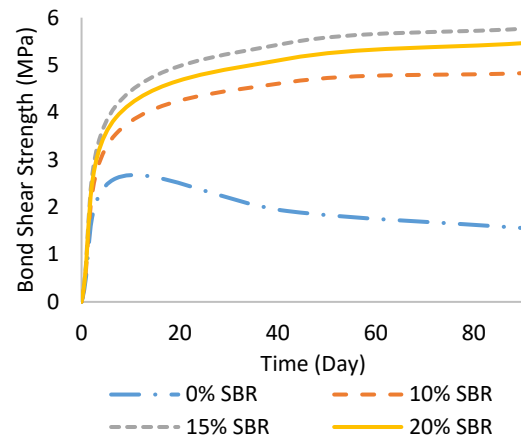


Fig. 13. Bond shear strength

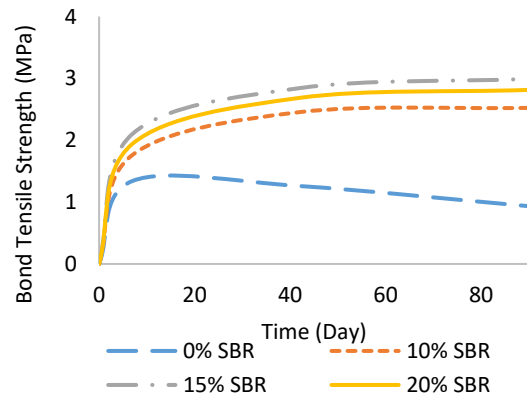


Fig. 14. Bond tensile strength

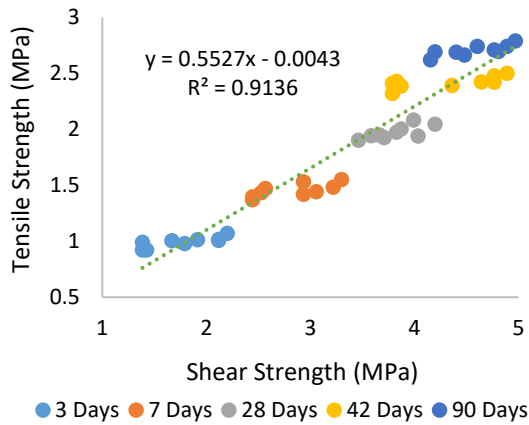


Fig. 15. The correlation between the results of “friction-transfer” and “pull-off” tests

According to the Figure. 15, the determination factor of “pull-off” and “friction-transfer” tests is 91%. Considering the high correlation factor of the results of “pull-off” and “friction-transfer” tests, it is possible to obtain the results of one test and consider it for the other test. Also, it is worth noting that the damages of two methods are negligible. However, unlike the “pull-off” test, in which we have to use of chemical adhesives for attaching the metal cylinder to the mortar surface, all the employed instruments are mechanical in the “friction-transfer” test therefore, it has the unique application for each type of laboratory and environmental conditions. Also, it can be used without any humidity and thermal constraint. Therefore, the simple and cheap machine of the “friction-transfer” test can be used instead of the expensive machine of the “pull-off” test for determining the bond strength between the concrete substrate and the polymer-modified mortars.

Other studies have obtained similar results. A study has mentioned that the correlation coefficients of more than 93% exist between the friction-transfer and the pull-off test results for ordinary mortars [28].

3.4. Evaluating the effect of polymers on flexural and compressive strengths

This section discusses the effect of styrene-butadiene polymers on the compressive and flexural strengths of repair mortars. As stated previously, the 28-day compressive strength of the concrete substrate was 57 MPa. Table 4 provides the compressive and flexural strengths of the mortars.

As can be seen, the compressive and flexural strengths of the mortars have been increased by the completion of the hydration process due to the rise in the age of the specimens. Adding the styrene-butadiene rubber increased the flexural strength of the mortars. Therefore, in comparison with ordinary mortars, the 7-day flexural

strengths of the mortars modified with 10%, 15%, and 20% polymers have been increased by 18.1%, 38.6%, and 44.9%, respectively. Similar rises were observed at other ages as well. However, the addition of the polymer reduced the compressive strength of the mortars. In specific, the 7-day compressive strengths of those modified with 10%, 15%, and 20% polymers were decreased by 24.9%, 30.2%, and 33.1%, respectively. Similar observations were also witnessed for other ages. Also, in other studies have obtained similar results. As reported in [41], the styrene-butadiene rubber delayed the hydration process and reduced the compressive strength. Furthermore, the addition of the SBR to the mortar increased the air bubbles and porosity in the mortars, which directly reduced their compressive strengths. Another article reported an increased adhesion between the cement paste and aggregates by adding the styrene-butadiene rubber, which consequently yielded higher flexural strengths [44].

The SEM images of the specimens were obtained to evaluate their microscopic structures. Fig. 16 illustrates the microscopic image of the mortar containing SBR. As can be seen, the added SBR polymer in the mortar structure filled the cracks and prevented widening. As shown in Fig. 17, to make a better assessment, the diameter distribution of the SBR polymers in the mortar, along with their distribution histograms, were plotted using the Image J and Origin software programs. As can be seen, the most frequent diameter of the polymers was approximately 0.1 μm. Table 5 lists the statistical parameters of the measurement.

Table 4. The compressive strength of the mortars (MPa)

	SBR (%)	7 Days	42 Days	90 Days
Compressive strength	0%	34.1	51.2	54.4
	10%	25.6	38.8	42.2
	15%	23.8	37.7	40.8
	20%	22.8	36.1	39.2
Flexural strength	0%	8.6	9.71	10.11
	10%	10.51	12.02	12.55
	15%	11.92	13.52	14.19
	20%	12.46	14.54	15.2

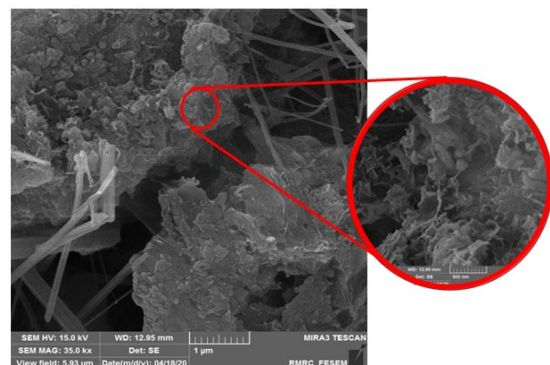


Fig. 16. Microscopic image of the mortar containing SBR

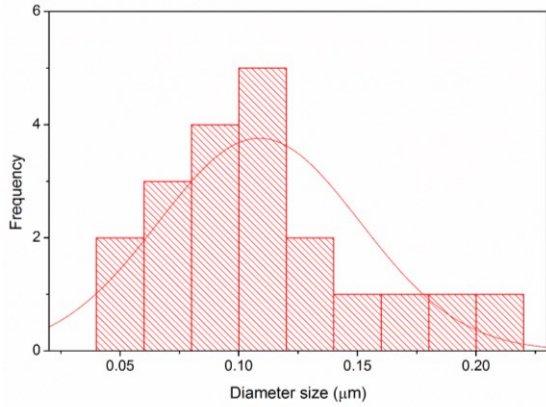


Fig. 17. The diameter distribution histogram of the SBR polymer in the mortar

Table 5. Statistical parameters obtained from the diameter distribution of SBR fibers in the mortar

Number of measurements	Mean size (μm)	The smallest measured diameter (μm)	The largest measured diameter (μm)
20	0.098	0.053	0.201

As shown in Table 5, the mean diameter of the polymers was approximately 98nm. Therefore, they could be considered nanoparticles due to having diameters lower than 100nm. Moreover, the smallest and largest measured diameters were 53nm and 201nm, respectively. Nanoparticles of the material have unique properties, which cannot be observed in larger particles of the same material. Thus, the reduced nanometric diameter of the polymers has improved the properties of the bond between the mortar and the substrate.

3.5. Modeling the “friction-transfer” and “pull-off” tests

ABAQUS provides brittle cracking, smeared cracking, and concrete damage plasticity models to consider the nonlinear behavior of brittle materials. The concrete damage plasticity model supports static and dynamic analyses with tensile cracking and compressive crushing mechanisms. Since by imposing a torsional moment in a friction-transfer test, the core is subjected to compressive and tensile forces, this study used the concrete damage plasticity model for modeling.

In order to model the friction-transfer and pull-off tests, the cubic mortar piece was meshed using a combination of C3D8R and C3D4 elements. The main part of the model, which was under compression or tension, was meshed using C3D8R 8-node cubic elements with reduced integration. The convergence of meshes with sizes of 0.5, 1, and 2 mm was evaluated, among

which 1-mm meshes were chosen to be used in the modeling.

The important point in the meshing of the specimens is convergence. The results obtained from solving a problem in the FEM are always dependent on the size of the meshes and the size of the elements used. The problem-solving converges to a single solution by reducing the dimensions of the elements. However, the meshing size improvement should be done so as not to cause a sharp increase in computational volume. Since finite element solutions are dependent on the meshing size, the meshing convergence must always be checked in areas of the model where the values of stress, strain, or any other parameter must be accurately calculated. The meshing size can be considered large enough in areas far from stress concentration points.

As it can be seen in Figure 18, the modeling is performed with different kinds of meshing. The results were highly changed by decreasing the elements from 2 to 1 mm. Although, it can be observed that the value of maximal responses will be very close together by changing the size of the element from 1 to 0.5 mm. It was therefore decided to use meshing with the size of 1 mm.

Moreover, the edges were meshed using tetrahedral 4-node continuous elements with a minimum element size of 1 mm in the areas connected to the major elements, and a maximum element size of 15 mm on the edges. In the pull-off test, the adhesive was meshed with 2-mm C3D8R elements, and the mesh size of the steel piece was also 2 mm. along the axial direction, 10-mm meshes were used for the steel piece (Fig. 19).

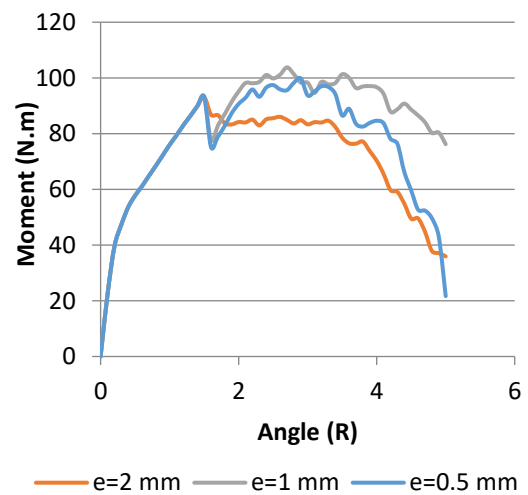


Fig. 18. Mesh sizing sensitivity

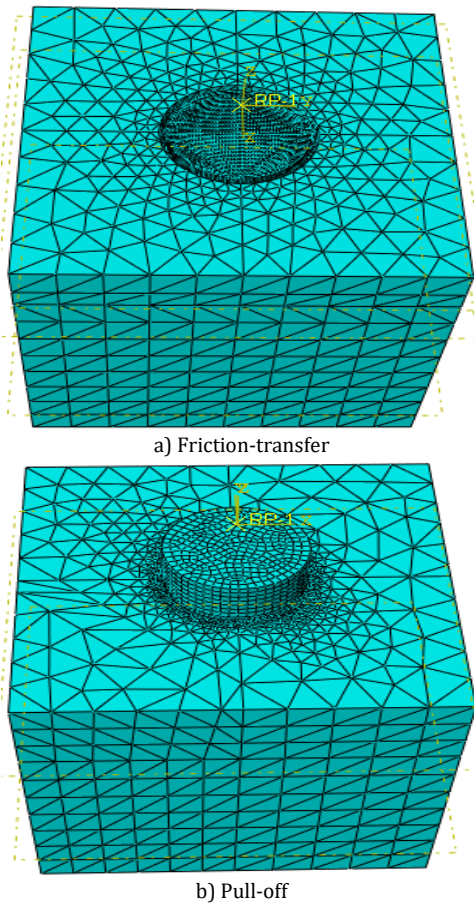


Fig. 19. The meshing of the specimens

The specimens were braced inside a steel frame to perform the friction-transfer tests. The bracing section had a height of 30 mm from the bottom of the specimen. As shown in Fig. 20.a, the bottom part of the specimen was defined as a support in the modeling. In the pull-off test, since the apparatus was placed on the top surface of the specimen in the laboratory, the top part of the specimen was defined with boundary conditions in the modeling (Fig. 20.b).

In order to define the behavior of the concrete after cracking under tension, with respect to the default mode of the program, the compressive hardening recovery, w_c , was considered "one" to completely recover the compressive hardening while the cracks were getting closed (after cracking under tension). On the other hand, w_t was considered "zero" to ignore the tensile hardening recovery.

The default values of the program were also considered for the plasticity properties of the concrete (Table 6). The dilation angle is a parameter in degrees, which depends on the materials' density and angle of internal friction. The eccentricity is a small positive value indicating the closeness rate of a hyperboloid to its asymptote. The third item in the Table 6 is the performance ratio of the biaxial initial stress to the uniaxial initial stress, and K denotes the ratio

of the second tensile stress to the compressive stress.

In order to build the model and introduce the materials' properties, the specimen parts were created at first using the "Create part" command. In order to model the concrete part using the "Create line" command, the rectangle of the concrete's cross-section was plotted, and its depth was defined as 150 mm. The "Create circle" command was used to plot the steel part and the adhesive. The "Property" module was used to define the materials' properties. Table 7 lists the properties of the used materials.

Afterward, the materials were assigned to the parts by using the commands "Create section" and "Assign section". In the "Plasticity" item, the "Concrete damaged plasticity" option was selected to define the plasticity properties. The compressive and tensile behaviors were then defined in the "Compressive behavior" and "Tensile behavior" sections. Afterward, the parts were assembled using the "Assembly" command.

As shown in previous sections, in the friction-transfer test, a metal piece was placed around the mortar core, which was fixed with the surrounding bolts, and enclosed the core. In order to evaluate the effects of lateral pressures applied by the metal piece on the core on the results, various lateral pressures were imposed on the core. As shown in Fig. 21, by clicking on the "Pressure" option in the "Load" item, the core's edges were selected, subjected to various pressures, and then analyzed.

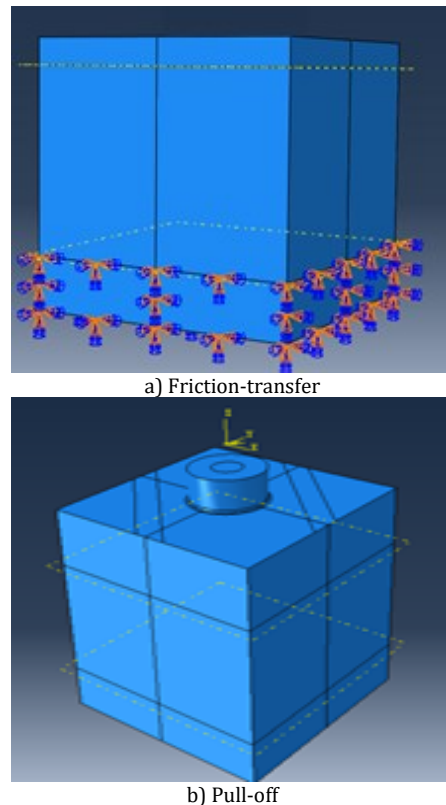


Fig. 20. Boundary conditions

Table 6. The plasticity properties of the concrete

Dilation angle ψ	Eccentricity ϵ	σ_{b0}/σ_{c0}	K	Viscosity
36	0.1	1.16	0.667	0

Table 7. The properties of the adhesive and the steel

Material	Young module (MPa)	Poisson's ratio	Density ton/mm^3
Adhesive	12556	0.49	2000×10^{-12}
Steel	210000	0.3	7800×10^{-12}

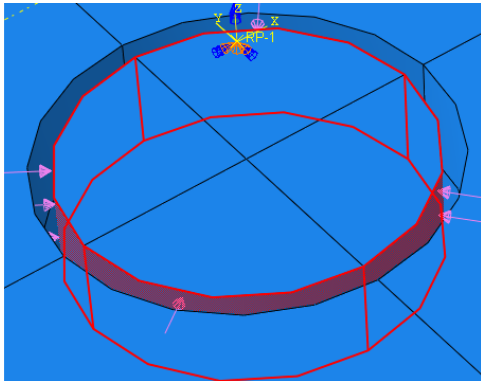


Fig. 21. The pressure of the metal piece on the core

Applying various pressures did not lead to a significant change in the results. Therefore, in order to model the interaction between the metal piece and the core in the friction-transfer test, a torsional moment was applied to the core perimeter in the form of a rotational displacement around the core axis using the coupling constraint, as shown in Fig. 22. To do so, a reference point was created on top of the core using the item “Tools” and choosing the option “Reference point”. Then, a coupling constraint was imposed in the “Interaction” section, and the areas around the core interacting with the metal core were chosen as the controllable part.

A mortar with a compressive strength of 47.6 MPa was used to model the specimens. The results of the friction-transfer and pull-off tests on the abovementioned specimen in the laboratory were 115 Nm and 4500 N, respectively.

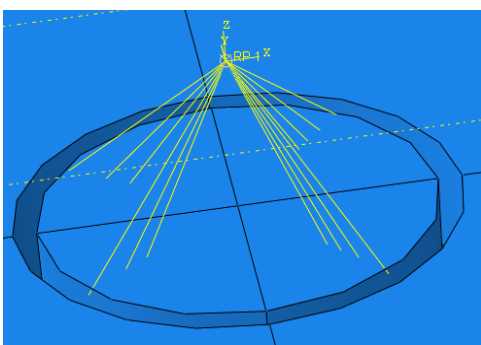


Fig. 22. Modeling the interaction between the metal piece and the mortar

When modeling the friction-transfer test, the cracks appeared on the edges and corners of the specimen, subjected to the largest stress, at the moment of 54 Nm. Then, at the moment of 107 Nm, the cracks reached each other, and the specimen failed (Fig. 23). By comparing the results of modeling and the experimental results it is obvious that the sample fracture in the “friction-transfer” test occurs in both cases as 45 degrees. Since, based on the Mohr circle the main compressive and tensile stresses make a 45 degrees angle with the horizon. Considering that the brittle materials such as mortar have the tensile fracture, therefore, in this case, the fracture planes appear to be vertical to the tensile stress. Therefore, in the “friction-transfer” test, the core fracture has an angle of about 45 degrees with the horizon.

When modeling the pull-off test, the first cracks appeared on the edges of the connection between the steel cylinder and the specimen at the force of 2448 N. Then, the cracks reached each other, and the specimen failed at the force of 1555 N (Fig. 24).

In order to verification the modeling results obtained from ABAQUS and to make a detailed comparison between the numerical and experimental results, they are provided in the following. Table 8 presents the results obtained from the modeling, the friction-transfer test, and the pull-off test.

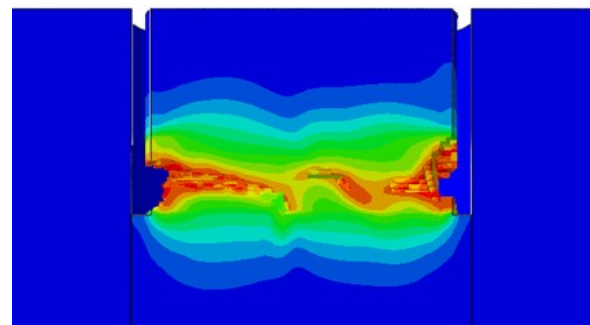


Fig. 23. The moment of failure in the friction-transfer test

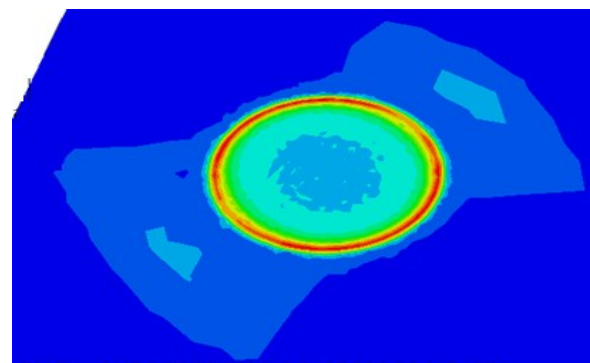


Fig. 24. The moment of failure in the pull-off test

Table 8. The numerical and experimental results of the friction-transfer test

Test	Numerical results	Experimental results	Difference between the results (%)
Friction-transfer (Nm)	107	115	7
Pull-off (N)	4555	4500	2

As can be seen, the differences between the modeling results and those obtained from the friction-transfer and pull-off tests in the laboratory were smaller than 7% and 2%, respectively.

4. Conclusions

In this paper, regression analysis was used to determine the correlation between the measurements of the semi-destructive tests and the results obtained for the compressive and flexural strength of the mortars. Furthermore, calibration curves were developed to obtain the mechanical properties of the mortars. The effects of the polymer on the shrinkage and the bond strength between the mortars and the concrete substrate were also investigated. Eventually, the stresses and cracks formed in the friction-transfer and pull-off tests were obtained through finite element analysis in ABAQUS. The results are as follows:

- The styrene-butadiene rubber increased the shear and bond tensile strength between the repair mortars and the concrete substrate. The largest rise in the shear and bond tensile strength (i.e., 269.9% and 220.3%, respectively) belonged to the mortar containing 15% polymer.
- The styrene-butadiene rubber reduced the shrinkage of the mortars, which is an important factor in increasing the adhesion between the mortar and the concrete. At the age of 14 days, the addition of 10%, 15%, and 20% SBR reduced the shrinkage by 32.8%, 36.1%, and 42.1%, respectively.
- Given the high correlation between the friction-transfer and pull-off tests, the low-cost and simple friction-transfer apparatus can be used instead of the imported pull-off apparatus to measure the adhesion between the mortar and the concrete.
- Due to the high correlation between the results of the in-situ tests and the compressive and flexural strengths of the mortars, the abovementioned tests can be used for evaluating the strength of the polymer-modified mortars.

- The styrene-butadiene rubber latex had a positive effect on the flexural strength of the mortars, i.e., adding 20% polymer increased the 90-day flexural strength by 50.3%.
- The results obtained from the finite element analysis in ABAQUS had a good agreement with those obtained in the laboratory, confirming the high accuracy of the semi-destructive tests for evaluating the strength of the mortars.

References

- [1] Ahmed, S.A., Hawraa, S.J. and Inas, S.M., 2012. Improvement the properties of cement mortar by using styrene butadiene rubber polymer. *Engineering and Development*, 16(3), pp.61-72.
- [2] Shuyi, Y. and Yong, G., 2012. Effect of styrene butadiene rubber latex on mortar and concrete properties. *Advanced Engineering Forum*, 5(1), pp.283-288.
- [3] Knapen, E. and Gemert, D., 2015. Polymer film formation in cement mortars modified with water-soluble polymers. *Cement and Concrete Composites*, 58(7), pp.23-28.
- [4] Qizheng, D., Lianjun, Ch., Weimin, Ch., Zhaoxia, L., Xiangfei, C., Guoming, L., Zhiwei, Sh., Zhenjiao, S. and Yaqing, Z., 2020. Material performance tests of the polymer-cement thin spray-on liner. *Geofluids*, 20(2), pp.1-14.
- [5] Çavdar, A., Sevin, S., Kaya, Y. and Bingöl, Ş., 2014. The effects of cure conditions on mechanical properties of polymer modified cement mortars. *Balkan Journal of Electrical and Computer Engineering*, 2(2), pp.79-85.
- [6] Doğan, M. and Bideci, A., 2016. Effect of styrene butadiene copolymer admixture on high strength concrete. *Construction and Building Materials*, 112(1), pp.378-385.
- [7] Afridi, M.U.K., Ohama, Y., Zafar, M. and Demura, K., 1995. Water retention and adhesion of powdered and aqueous polymer-modified mortars. *Cement and Concrete Composites*, 17(3), pp.113-118.
- [8] Tsai-Lung, W., 2017. Evaluation of cementitious repair mortars modified with polymers. *Advances in Mechanical Engineering*, 9(1), pp.1-7.
- [9] Zhihang, W., Jinyu, X., Wei, X., Zhe, H., Xin, M. and Xing, X., 2020. Research on interfacial bonding properties and engineering applications of polymer modified mortar. *E3S Web of Conferences*, 198(4), pp.23-27.
- [10] Min-Ook, K., 2020. Influence of polymer types on the mechanical properties of polymer-

modified cement mortars. *Applied Sciences*, 10(3), pp.1-12.

[11] Sadrmomtazi, A. and Khoshkbigari, R., 2019. Determination and prediction of bonding strength of polymer modified concrete as the repair overlay on the conventional concrete substrate. *KSCE Journal of Civil Engineering*, 23(3), pp.1141-1149.

[12] Joseph, J.A., Dana, N., Stephanie, Ch. and Tarek, T., 2020. Parametric study on polymer-modified pigmented cementitious overlays for colored applications. *Journal of Building Engineering*, 27(2), pp.1-13.

[13] Lin, L., Ru, W. and Qinyuan, L., 2018. Influence of polymer latex on the setting time, mechanical properties and durability of calcium sulfoaluminate cement mortar. *Construction and Building Materials*, 169(4), pp.911-922.

[14] Ali, A.M.Y., Mohammed, R.I. and Mahmoud, S.A., 2020. Physico-mechanical properties of irradiated SBR latex polymer-modified cement mortar composites. *Journal of Vinyl and Additive Technology*, 26(2), pp.144-154.

[15] Young, K., 2020. Adhesion in tension of polymer cement mortar by curing conditions using polymer dispersions as cement modifier. *Construction and Building Materials*, 242(1), pp.48-50.

[16] Sadrmomtazi, A. and Khoshkbigari, R.K., 2017. An investigation on in-situ strength and bonding strength of polymer modified concretes as repair overlays on conventional concrete substrate. *Journal of Rehabilitation in Civil Engineering*, 5(1), pp.67-78.

[17] Souza, M.H. and Souza, R.A., 2019. Analysis of compost repair mortars by vinyl copolymer PVA and SBR. *Revista Alconpat*, 9(3), pp.277-287.

[18] Kim, K.K., Yeon, J., Lee, H.E. and Yeon, J.H., 2019. Dimensional stability of SBR-modified cementitious mixtures for use in 3D additive construction. *Applied Sciences*, 9(16), pp.1-13.

[19] Hawileh, R.A., Rasheed, H., Abdalla, J.A. and Al-Tamimi, A., 2014. Behavior of reinforced concrete beams strengthened with externally bonded hybrid fiber reinforced polymer systems. *Materials and Design*, 53(2), pp.972-982.

[20] Salama, A.E., Ghanem, G.A. and Elnaby, M., 2012. Behavior of thermally protected RC beams strengthened with CFRP under dual effect of elevated temperature and loading. *HBRC Journal*, 8(1), pp.26-35.

[21] Mostofinejad, D., Esfahani, M.R. and Shomali, A., 2019. Experimental and numerical study of the RC beams shear-strengthened with NSM technique. *Journal of Composite Materials*, 53(17), pp.2377-2389.

[22] Abdalla, S., Al-Aama, N. and Al-Ghamdi, M., 2017. A Bio polymeric adhesive produced by photo cross-linkable technique. *Polymers*, 9(8), pp.1-18.

[23] ASTM International., 2018. ASTM C808/C805M-18: Standard test method for rebound number of hardened concrete. In Annual book of ASTM standards. West Conshohocken, PA: American Society for Testing and Materials, p.4.

[24] ASTM International., 2016. ASTM C597-16: Standard test method for pulse velocity through concrete. In Annual book of ASTM standards. West Conshohocken, PA: American Society for Testing and Materials, p.4.

[25] ACI Committee 214, Report 214.4R-03., 2003. Guide for obtaining cores and interpreting compressive strength results, American Concrete Institute. p.16.

[26] ASTM International., 2015. ASTM C900-15: Standard test method for pullout strength of hardened concrete. In Annual book of ASTM standards. West Conshohocken, PA: American Society for Testing and Materials, p.10.

[27] ASTM International., 2004. ASTM C1583: Standard test method for tensile strength of concrete surfaces and the bond strength or tensile strength of concrete repair and overlay materials by direct tension (pull-off method). In Annual book of ASTM standards. West Conshohocken, PA: American Society for Testing and Materials, p.5.

[28] Naderi, M., 2005. Friction-transfer test for the assessment of in-situ strength and adhesion of cementitious materials. *Construction and Building Materials*, 19(6), pp.454-459.

[29] Naderi, M., 2007. New twist-off method for the evaluation of in-situ strength of concrete. *Journal of Testing and Evaluation*, 35(6), pp.602-608.

[30] ASTM International., 2015. ASTM C128-15: Standard test method for relative density (Specific gravity) and absorption of coarse aggregate. In Annual book of ASTM standards. West Conshohocken, PA: American Society for Testing and Materials, p.6.

[31] ASTM International., 2015. ASTM C127-15: Standard test method for relative density (Specific gravity) and absorption of fine aggregate. In Annual book of ASTM standards. West Conshohocken, PA: American Society for Testing and Materials, p.5.

[32] ASTM International., 2001. ASTM C136-01: Standard test method for sieve analysis of fine and coarse aggregates. In Annual book of ASTM

standards. West Conshohocken, PA: American Society for Testing and Materials, p.5.

[33] BHRC publication., 2008. The national method for concrete mix design. Building and Housing Research Center, No. S-479, p.50.

[34] ASTM International., 2008. ASTM C157: Standard test method for length change of hardened hydraulic cement mortar and concrete. In Annual book of ASTM standards. West Conshohocken, PA: American Society for Testing and Materials, p.8.

[35] ASTM International., 2011. ASTM C490: Standard practice for use of apparatus for the determination of length change of hardened cement paste, mortar, and concrete. In Annual book of ASTM standards. West Conshohocken, PA: American Society for Testing and Materials, p.5.

[36] ASTM International., 2013. ASTM C109: Standard test method for compressive strength of hydraulic cement mortars (using 2-in. or [50-mm] cube specimens). In Annual book of ASTM standards. West Conshohocken, PA: American Society for Testing and Materials, p.10.

[37] ASTM International., 1985. ASTM C190: Standard test method for tensile strength of hydraulic cement mortars. In Annual book of ASTM standards. West Conshohocken, PA: American Society for Testing and Materials, p.6.

[38] Diab, A.M., Elyamany, H.E. and Ali, A.H., 2013. Experimental investigation of the effect of latex solid/water ratio on latex modified co-matrix mechanical properties. *Alexandria Engineering Journal*, 52(2), pp.83-98.

[39] Baoshan, H., Hao, W., Xiang, Sh. and Burdette, E.G., 2010. Laboratory evaluation of permeability and strength of polymer-modified pervious concrete. *Construction and Building Materials*, 24(5), pp.818-823.

[40] Jiang, H.Y. and Liu, Z.X., 1996. Research of polymer cement concrete. *Journal of Wu Han University of Technology*, 18(2), pp.37-38.

[41] Tian, Y., Jin, X.Y., Jin, N.G., Zhao, R., Li, Z.J. and Ma, H.Y., 2013. Research on the microstructure formation of polyacrylate latex modified mortars. *Construction and Building Materials*, 47(1), pp.1381-1394.

[42] Ohama, Y., 1995. Polymer modified concrete mortars-properties and process technology. Noyes, United States of America. ISBN: 9780815517696. p. 246.

[43] Czarnecki, L. and Sokolowska, J.J., 2015. Material model and revealing the truth. *Bulletin of the Polish Academy of Sciences Technical Sciences*, 63(1), pp.7-14.

[44] Rossignolo, J.A., 2009. Interfacial interactions in concretes with silica fume and SBR latex. *Construction and Building Materials*, 23(2), pp.817-821.